PROCEEDINGS OF SCIENCE

Recent Spectroscopy Highlights from COMPASS

Henri Clemens Pekeler[*a,*]

[a] *Helmholtz-Institut für Strahlen- und Kernphysik, Universität Bonn, Germany*

E-mail: henri.pekeler@cern.ch

The COMPASS experiment took data at the M2 beam line at CERN with a rich hadron physics program for the last two decades. This talk focuses on the spectroscopy program, where a 190 GeV negatively charged hadron beam was shot on a fixed proton target.
We investigate diffractive dissociation events in various final states using both the π^- and K^- component of the beam. Performing a partial-wave decomposition and fitting resonance models allows us to measure a_J, π_J, K_J and K_J^* states and to extract their resonance parameters.
Especially exciting are exotic mesonic states beyond the $q\bar{q}$ systematics of up, down and strange quarks. An example are hybrid states where gluonic degrees of freedom contribute to the quantum numbers. Models as well as recent lattice QCD simulations predict the lightest hybrid state to have spin-exotic quantum numbers $J^{PC} = 1^{-+}$. A coupled-channel fit to COMPASS data using selected $\eta\pi$ and $\eta'\pi$ final states results in 1^{-+} signals at different masses originating from a single pole at about $1.6\,\mathrm{GeV}/c^2$.
In addition, we show recently released results for the $\omega\pi^-\pi^0$ final state, confirming the $\pi_1(1600)$, as well as other known states.
The strange-light sector is probed with the reaction $K^-p \to K^-\pi^-\pi^+p$, where COMPASS selected the largest data set to date and we show results for known states as well as new states, e.g. an exotic 0^- candidate.

Supported by BMBF.

16th International Conference on Heavy Quarks and Leptons (HQL2023)
28 November-2 December 2023
TIFR, Mumbai, Maharashtra, India

[*] talk given on behalf of the COMPASS Collaboration
[*] Speaker

1. Introduction

Recent lattice calculations [1] as well as several effective models (flux tube, bag) predict the lightest hybrid meson to have quantum numbers 1^{-+}. The lattice calculations predict $b_1\pi$ as the most dominant decay of the hybrid meson, with weaker contributions of $f_1(1285)\pi$, $\rho\pi$, $\eta'\pi$, $\eta\pi$ and others. Searches for this hybrid meson are ongoing since many years [2–4] and for the longest time, there was the puzzle between the $\pi_1(1400)$ and $\pi_1(1600)$ as candidates for the lightest hybrid meson, while only one state is predicted by theory.

All final states listed above (and more) can be investigated by the COMPASS experiment, within its hadron spectroscopy program.

2. Resonance searches at COMPASS

The **CO**mmon **M**uon **P**roton **A**pparatus for **S**tructure and **S**pectroscopy had many different physics programs from 2002-2022. Amongst them were two years of dedicated data taking for light-meson spectroscopy with diffractive hadron proton scattering. COMPASS is a fixed target experiment located at the **S**uper **P**roton **S**ynchrotron at CERN. Via the M2 beamline a beam of negatively charged particles with a momentum of 190 GeV/c is selected with a pion (96.8%), kaon (2.4%) and anti-proton (0.8%) component. The reaction of interest is given by $h^-p \to X^-p$, where the intermediate state X^- is formed predominantly via Pomeron exchange in the t-channel and decays to hadrons, which are measured by the spectrometer.

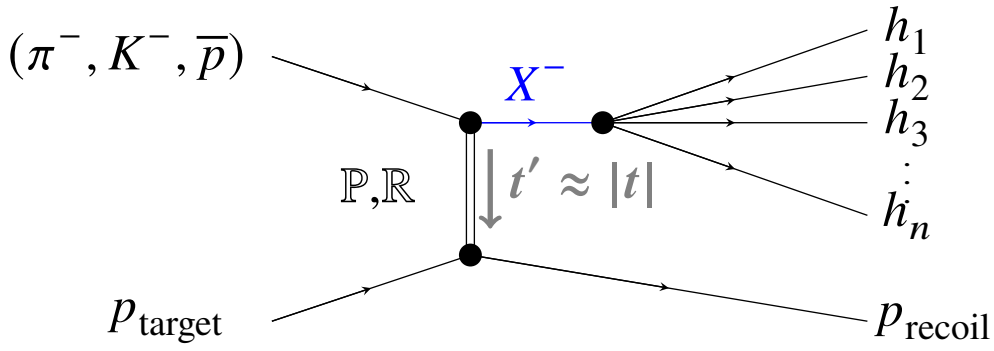

Figure 1: General diagram of diffractive hadron-proton scattering, analyzed by COMPASS.

This diffractive scattering process can be subdivided into two processes. The first one describes the inelastic scattering of the beam particle with the target proton, leaving the proton intact and creating some excited pion or kaon state X^-, followed by the decay of the excited state X^- to hadrons. The first stage can be characterized by the Mandelstam variables s and t as well as the mass of X^-. In general, the momentum transfer t can be described as follows

$$t = (p_1 - p_3)^2 = m_1^2 + m_3^2 - 2(E_1E_3 - |\vec{p}_1||\vec{p}_3|\cos\theta_{13}) \tag{1}$$

with the first particle being the beam particle, the second one is the target proton, the third one is the resonance X^- and the fourth one is the recoil proton. In the center-of-momentum frame, we

can calculate the energy via

$$E_{1,\mathrm{CM}} = \frac{s + m_2^2 - m_1^2}{2\sqrt{s}}. \tag{2}$$

With $\cos\theta_{13} = \pm 1$, the minimum and maximum values of t in the center-of-momentum frame are

$$t^{\mathrm{CM}}_{\mathrm{min,max}} = m_1^2 + m_3^2 \mp 2\left(E_{1,\mathrm{CM}}E_{3,\mathrm{CM}} - \sqrt{E_{1,\mathrm{CM}}^2 - m_1^2}\sqrt{E_{3,\mathrm{CM}}^2 - m_3^2}\right). \tag{3}$$

These values exhibit an event-by-event bias which we can correct for by introducing the variable t' as

$$t' = |t| - \left|t_{\mathrm{max}}\right| \tag{4}$$

and use it instead of t to describe the kinematics. The second stage of the reaction is described via subsequent two-body decays employing the isobar model. We model the three body decay of X^-, (see sec. 5 and 6), with a decay into a two-body resonance - called isobar - and a bachelor particle. Then, the isobar decays further into the remaining final-state particles (see fig. 2).

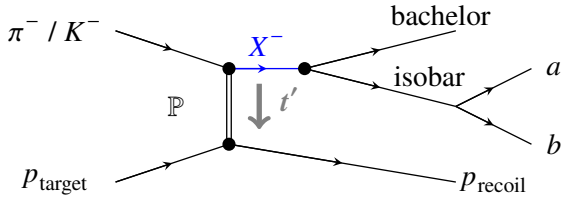

Figure 2: Representation of the reaction $\pi^-/K^-p \to X^-p$, $X^- \to$ three hadrons, in the isobar model. The decay of X^- is modeled as two two-body decays. First, it decays to a bachelor particle and an isobar, then the isobar decays to two hadrons a and b.

Additionally, a decomposition of the decay amplitude into partial waves, containing only contributions from a single decay channel and one specific set of resonance quantum numbers, is performed, where a truncation of the in principle infinite sum is done by exploiting phase-space arguments and other techniques to reasonably decrease the number of partial waves. We present this briefly in sec. 3. For a more detailed description on these techniques see [5, 6].

3. Partial-wave-analysis technique

The ultimate goal of the partial-wave analysis is to characterize the intermediate state X^- for a given exclusive final state, e.g $\eta^{(\prime)}\pi^-$ (see sec. 4), $\omega\pi^-\pi^0$ (see sec. 5) or $K^-\pi^+\pi^-$ (see sec. 6). More precisely, we want to decompose our data into contributions from different partial waves, each of them describing different decay modes and / or representing different final state quantum numbers. A parametrization of the decay amplitudes for the partial waves can be found in [6].

We split our data in bins of t' and m_X and build an intensity function per bin, consisting of the coherent sum over all partial waves, each of them multiplied by a complex fit parameter. These fit parameters are identified as the transition amplitudes, i.e. a measure of how prominent a given partial wave is via its absolute value and a measure of the interplay between partial waves via the relative phase between two transition amplitudes, of the given partial wave and the given (m_X, t') bin.

Given the constructed intensity, we extract the transition amplitudes with an extended-likelihood fit.

In the second stage of the analysis, we fit these m_X and t' dependent transition amplitudes to extract resonance parameters (masses and width) together with background components. Naturally, the resonance parameters should be independent of t'. However, the background has an explicit t' dependence. Therefore, it is important to choose the bins narrow enough in order to ensure that we can separate the background from the resonant components.

4. Results in the $\eta^{(\prime)}\pi^-$ final state

For a long time, there was a puzzle about the $\pi_1(1400)$ and $\pi_1(1600)$ states. Different experiments (see [2, 3]) have reported a signal in the spin-exotic $J^{PC} = 1^{-+}$ partial wave. When they looked into the $\eta\pi^-$ final state, they saw a peaking structure around 1.4 GeV/c^2 and in the $\eta'\pi^-$ final state they saw a structure around 1.6 GeV/c^2. COMPASS has published (see [4]) its finding in the $\eta\pi^-$ and $\eta'\pi^-$ final states and observed structures in the same regions (see fig. 3). In order to compare the results in the $\eta\pi^-$ and $\eta'\pi^-$, we take into account their different phase spaces and angular-momentum barriers in fig 3b. Within the partial-wave decomposition, we have vanishing intensity in the $\eta\pi^-$ P-Wave between 1.8 GeV/c^2 and 2 GeV/c^2, which leads to an ill-defined phase between the P- and D-Wave, shown as a gray area in fig. 3c.

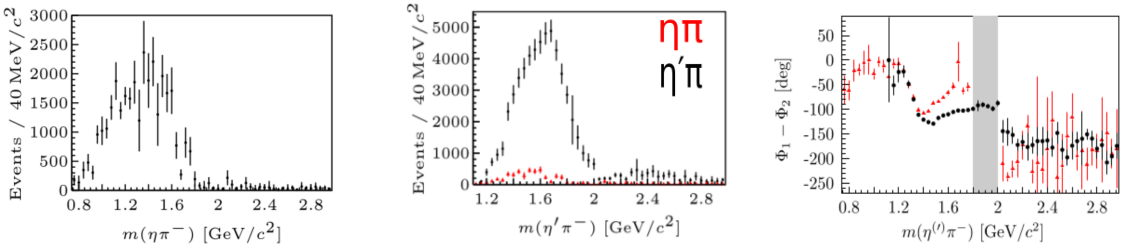

(a) Intensity of the P-wave for $\eta\pi^-$.

(b) Intensity of the P-wave for $\eta\pi^-$ and $\eta'\pi^-$, scaled by phase space.

(c) Relative phase of the P- and D-wave for $\eta\pi^-$ and $\eta'\pi^-$.

Figure 3: Intensity and phase distribution of the $\eta\pi^-$ and $\eta'\pi^-$ final state at COMPASS. The ill-defined phase, due to vanishing P-Wave intensity in the $\eta\pi^-$ final state is grayed out. [4]

A recent coupled-channel analysis via the K-matrix formalism (see [7]) has shown, that both peaks can be described by a single pole in the complex plane, meaning that there is only one resonance describing both ($\eta\pi^-$ and $\eta'\pi^-$) P-wave structures. This analysis was cross checked, where also $\bar{p}p$-, π^-p- and $\pi\pi$-data from other experiments was included (see [8]). Therefore, the puzzle about the two peaks at different positions in the $\eta\pi^-$ and $\eta'\pi^-$ final state is solved. There is only one $\pi_1(1600)$ resonance.

5. Results in the $\omega\pi^-\pi^0$ final state

For the $\omega\pi^-\pi^0$ final state, we select exclusive events via identifying two negatively charged, two neutral and one positively charged pion. Hereby, we require that exactly one combination of

$\pi^-\pi^+\pi^0$ is originating from the ω, i.e. we make a tight cut around the ω mass in the three-pion invariant-mass spectrum. In ca. 15% of the events, more than one combination fits. In these cases we discard the event. Now, we can factorize the decay $X^- \to \pi^-\pi^0\pi^-\pi^+\pi^0$ into $X^- \to \omega\pi^-\pi^0$ and $\omega \to \pi^-\pi^+\pi^0$, where the ω decay is identical for all partial waves. The different decay typologies are shown in fig. 4. Either, the X^- decays to an $\omega\pi$ isobar and a bachelor π (see fig. 4a) or to a $\pi\pi$ isobar and a bachelor ω (see fig. 4b). Note, that for the $\omega\pi$ isobar, the negative and neutral pion may be used, yielding different charge contribution of the isobar. With their relative strength given by isospin symmetry, we combine these two possibilities into one decay typology of X^-.

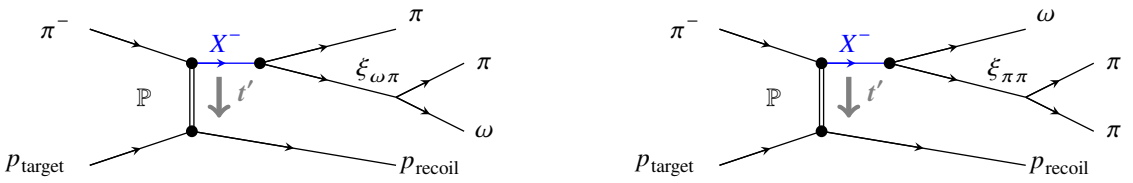

(a) $\omega\pi$ isobar **(b)** $\pi\pi$ isobar

Figure 4: Possible decay typologies in the isobar model for $\pi^- p \to X^- p$; $X^- \to \omega\pi^-\pi^0$

For this final state, we describe individual partial waves with the notation $J^P M^\epsilon [\xi l] b LS$. The quantum numbers of the state X^- are $J^P M^\epsilon$, where J is its total spin, P its parity, M the spin projection to the z-axis and the reflectivity ϵ that separates contributions from natural ($\epsilon = +$) and unnatural ($\epsilon = -$) exchanges (see [9] for a detailed description of the basis functions). LS describes the angular momentum and spin of the $X^- \to \xi b$ decay. ξ is the isobar and b the respective bachelor particle. l is the angular momentum of the decay of the isobar ξ.

The partial-wave decomposition is carried out in 4 t' bins and mass bins of 40 MeV/c^2 width. In the following, we will present results of the partial-wave decomposition in some partial-waves. A resonance signal will manifest itself as a peak in the intensity distribution, as well as a 180 deg phase motion in the relative phase of the partial wave. Of course, this only holds for a clean isolated resonance. A reduced phase motion might occur when there is more then one resonance and / or a background signal in the partial wave or the reference wave, with respect to which the relative phase is measured. A resonance-model fit to the intensities and phases is needed to clearly separate and identify the resonance signals. It is already in preparation.

We see clean, isolated signals in many partial waves and can make statements already without a resonance-model fit. In the $0^-0^+[\rho(770)P]\omega P1$ wave, we see a clean signal consistent with the $\pi(1800)$ (see fig. 5), in the $4^+1^+[b_1(1235)S]\pi F1$ partial wave, we see a clean signal consistent with the $a_4(1970)$ (see fig. 6) and in the $1^-1^+[b_1(1235)S]\pi S1$ partial wave we see a clean structure around the mass of the spin-exotic $\pi_1(1600)$, which matches our findings in the $\eta^{(\prime)}\pi$ (see sec. 4) and $\pi\pi\pi$ (see [10]) final state.

6. Results in the $K^-\pi^+\pi^-$ final state

The beam composition is dominated by pions. However, two **C**h**E**renkov **D**etectors with **A**cromatic **R**ing focus (CEDAR) within the M2 beam line that provides COMPASS with its beam particles, allow us to select the small kaon fraction in the beam and study diffractive production of

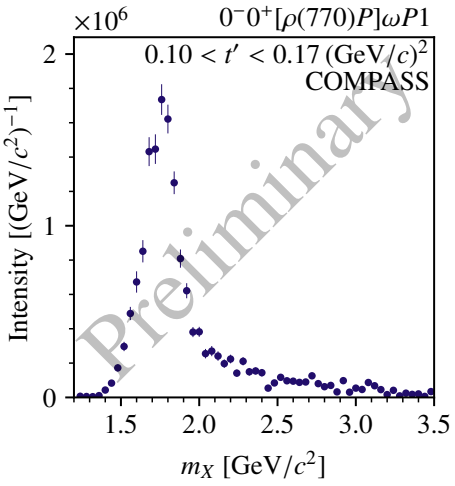

(a) Intensity distribution of the $0^-0^+[\rho(770)P]\omega P1$ partial wave.

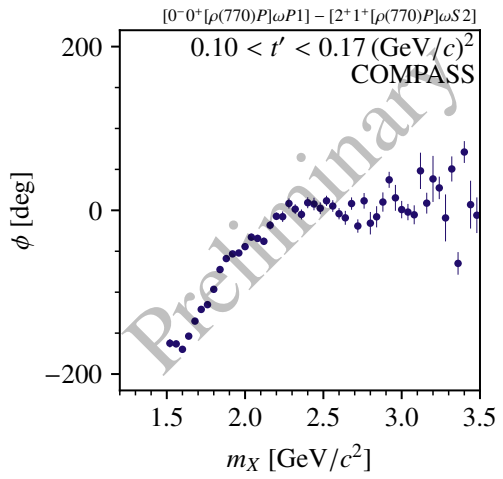

(b) Relative phase between the $0^-0^+[\rho(770)P]\omega P1$ partial wave and the $2^+1^+[\rho(770)P]\omega S2$ wave.

Figure 5: We see a clean signal consistent with the $\pi(1800)$ in the $0^-0^+[\rho(770)P]\omega P1$ wave, which shows itself via a strong peak in its intensity distribution and strong phase motion relative to the $2^+1^+[\rho(770)P]\omega S2$ reference wave.

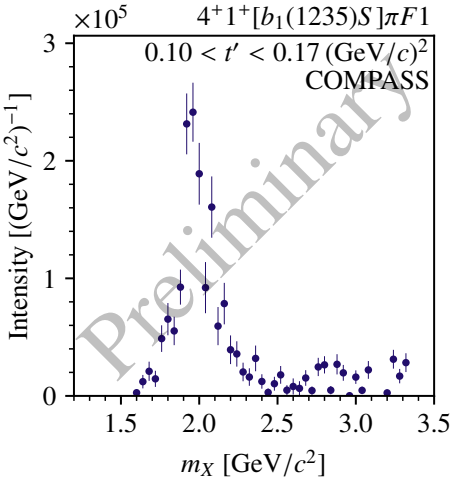

(a) Intensity distribution of the $4^+1^+[b_1(1235)S]\pi F1$ partial wave.

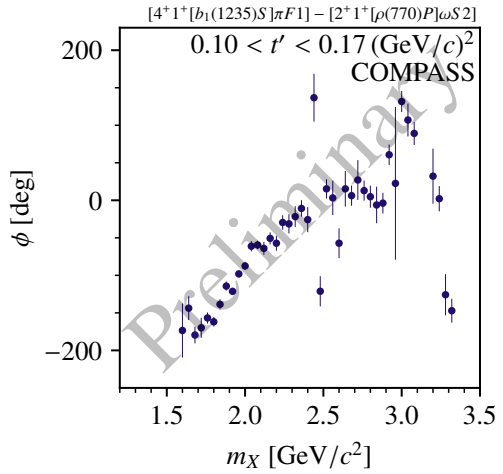

(b) Relative phase between the $4^+1^+[b_1(1235)S]\pi F1$ partial wave and the $2^+1^+[\rho(770)P]\omega S2$ wave.

Figure 6: We see a clean signal consistent with the $a_4(1970)$ in the $4^+1^+[b_1(1235)S]\pi F1$ wave, which shows itself via a strong peak in its intensity distribution and strong phase motion relative to the $2^+1^+[\rho(770)P]\omega S2$ reference wave.

strange-meson resonances. Within the COMPASS spectrometer, there is a **R**ing **I**miging **CH**erenkov detector (RICH), that can distinguish kaons and pions up to a momentum of about 60 GeV/c in the final state. However, the final-state particles have momenta up to the nominal beam momentum of 190 GeV/c. This incomplete kinematic coverage of our final-state PID causes understood

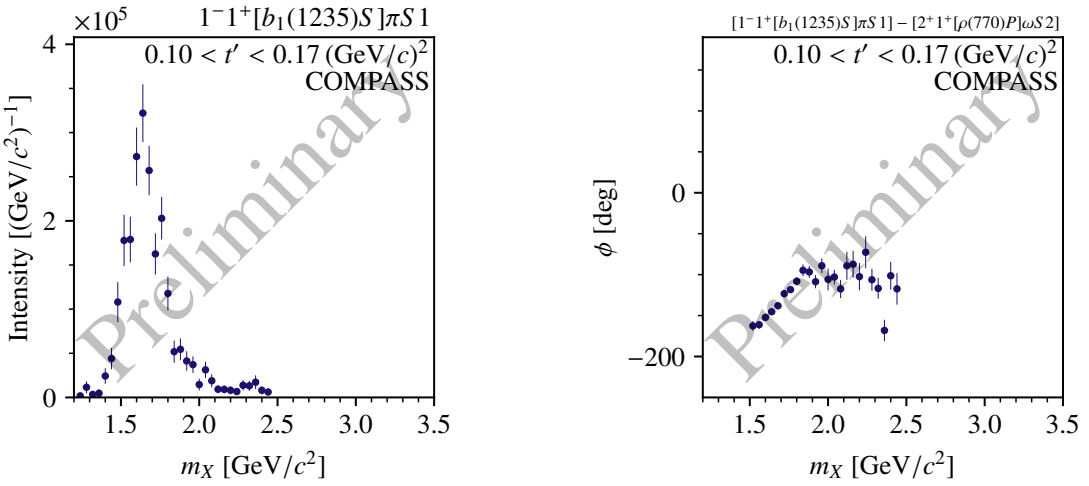

(a) Intensity distribution of the $1^-1^+[b_1(1235)S]\pi S1$ partial wave.

(b) Relative phase between the $1^-1^+[b_1(1235)S]\pi S1$ partial wave and the $2^+1^+[\rho(770)P]\omega S2$ wave.

Figure 7: We see a clean signal consistent with the spin-exotic $\pi_1(1600)$ in the $1^-1^+[b_1(1235)S]\pi S1$ wave, which shows itself via a strong peak in its intensity distribution and strong phase motion relative to the $2^+1^+[\rho(770)P]\omega S2$ reference wave.

backgrounds from other processes and analysis artifacts in the measured partial-wave amplitudes, which can for example be seen in fig. 10, where the partial wave depicted on the top left catches more intensity as expected in the low mass region. This leads to an inability to describe the peaks perfectly by the resonance-model fit. Systematic effects introduced by these imperfections were studied in detailed systematic and Monte Carlo input-output studies.

We characterize a partial wave via: $J^P M^\epsilon \xi^0 b^- L$, where $J^P M^\epsilon$ characterize the quantum numbers of X^- as for the $\omega\pi\pi$ final state. ξ^0 denotes the Isobar, b^- the bachelor particle and L is the orbital angular momentum between the Isobar and the bachelor. Note that we do not need more quantum number to describe the $K\pi\pi$ partial waves, mostly due to the fact, that all final state particles have zero spin and, therefore, the angular momentum in the decay of the isobar is clear, once J and L are detailed. You may see the decay typologies in fig. 8.

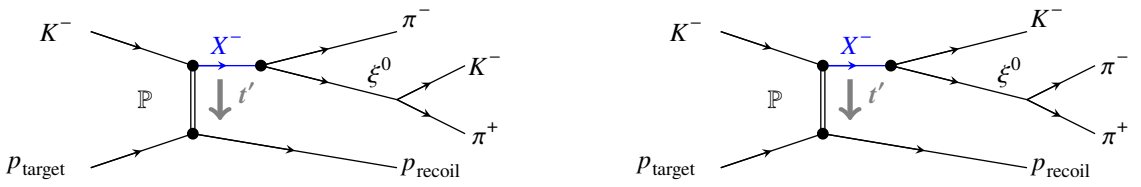

(a) $K\pi$ isobar

(b) $\pi\pi$ isobar

Figure 8: Possible decay typologies in the isobar model for $K^- p \to X^- p$; $X^- \to K^-\pi^-\pi^+$

In figure 9, we show a matrix plot of 3 partial waves. Clear peaks in the intensity as well as clear phase motion are visible. The resonance-model fit reproduces the peaking structure and phase motion at around 1.4 GeV/c^2 in the 2^+ sector with the $K_2^*(1430)$ resonance. Our estimates for the

parameters are: $m = (1430.9 \pm 1.4^{+3.1}_{-1.5})\,\mathrm{MeV}/c^2$ and $\Gamma = (111 \pm 3^{+4}_{-16})\,\mathrm{MeV}$, which match well with the values provided by the **P**article **D**ata **G**roup (PDG). Note, that the relative phase between the 2^+ waves and the reference wave drops at around $1.2\,\mathrm{GeV}/c^2$, due to the $K_1(1270)$, being present in the reference wave. The high-mass and low-mass tails of the 2^+ waves are mainly driven by model artifacts and are not correctly reproduced by the resonance-model fit. Therefore, we exclude them from the fit. We see no evidence for excited K_2^* resonances in the 2^+ sector.

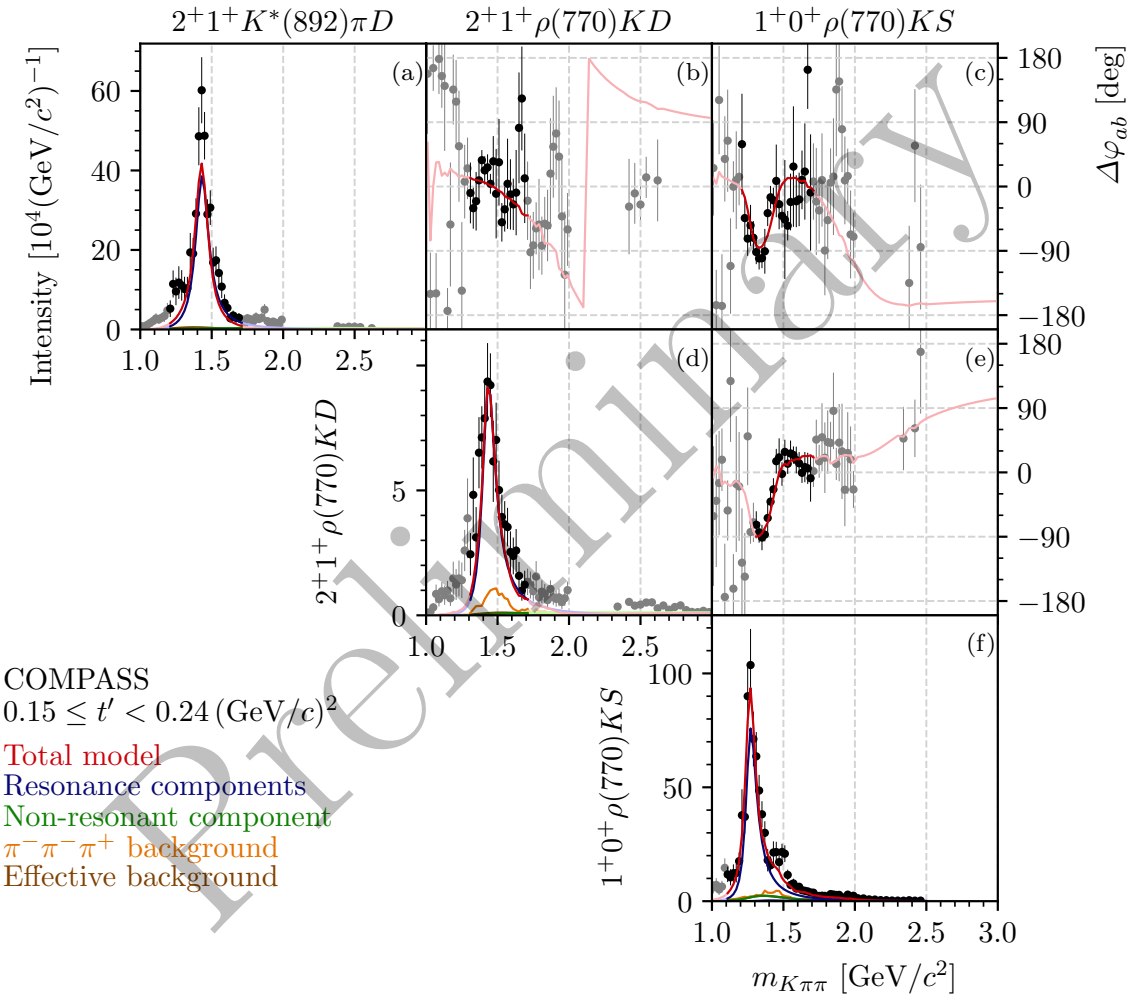

Figure 9: Matrix representation of the intensities of partial waves in the 2^+ sector, as well as the $1^+0^+\rho(770)KS$ reference wave and their relative phase. In addition we show the resonance model fit in red and its components in other colors.

In figure 10 we see a matrix plot for three partial waves. One of them is the interesting $0^-0^+\rho(770)KP$ wave. We see 3 peak like structures. One around $1.4\,\mathrm{GeV}/c^2$, one around $1.6\,\mathrm{GeV}/c^2$ and one around $1.8\,\mathrm{GeV}/c^2$. Within the resonance-model fit, we model the first peak by the $K(1460)$, the second one by the $K(1630)$ and the last by the $K(1830)$. Unfortunately, especially the first peak is not covered fully by the fit and we have seen in systematic studies that this is mostly due to the fact that the lower mass region in the partial-wave is affected from known analysis

artifacts, stemming from the incomplete kinematic coverage of the final-state PID. Still, once we fix the $K(1460)$ component to its PDG values within the resonance-model fit, we are able to describe the other two peaks and phase motions well, i.e. the $K(1630)$ with a statistical significance of 8.3σ and the $K(1830)$ with a statistical significance of 5.4σ. This is a very interesting result, since the quark-model predicts only two excited states in this mass region. We conclude, that we have evidence for a supernumerous state to the quark model, the $K(1630)$, since the other two states match best with the prediced quark-model states. This could, for example, be explained by a hybrid meson.

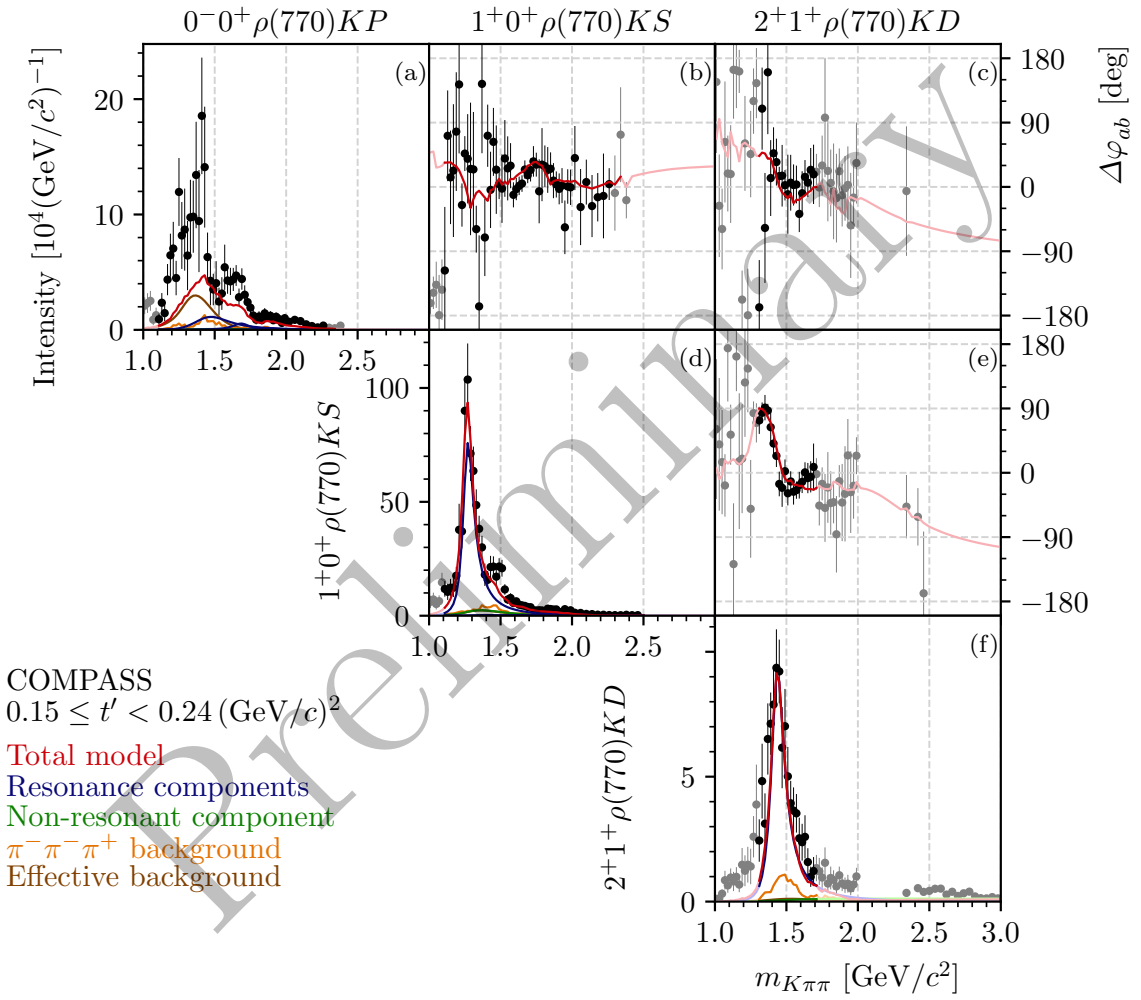

Figure 10: Matrix representation of the intensities of partial waves in the 0^- sector, the $1^+0^+\rho(770)KS$ reference wave and one wave in the 2^+ sector, as well as their relative phase. In addition we show the resonance model fit in red and its components in other colors.

7. Conclusion

COMPASS provides the world largest data set for diffractive pion-proton and kaon-proton scattering. We have shown that we can isolate the spin-exotic resonance $\pi_1(1600)$ in multiple final

states e.g. $\eta^{(\prime)}\pi^-$ and $\omega\pi^-\pi^0$ and that the long standing puzzle between the $\pi_1(1400)$ and $\pi_1(1600)$ is solved while using COMPASS data. There is only one pole in the complex plane needed to describe both signals as one $\pi_1(1600)$ resonance.

We have completed the full partial-wave analysis for the $K^-\pi^+\pi^-$ final state, confirming known states and yielding evidence for a supernoumerus state to the quark model in the pseudoscalar sector.

References

[1] Woss, A., et al., D. Decays of an exotic 1^{-+} hybrid meson resonance in QCD. *Phys. Rev. D.* **103**, 054502 (2021,3), https://link.aps.org/doi/10.1103/PhysRevD.103.054502

[2] Alde, D.,et al. Evidence for a 1^{-+} exotic meson. *Physics Letters B.* **205**, 397-400 (1988), https://www.sciencedirect.com/science/article/pii/0370269388916863

[3] Adams, G.,et al. Observation of a New $J^{PC} = 1^{-+}$ Exotic State in the Reaction $\pi^- p \to \pi^+\pi^-\pi^- p$ at $18\,\mathrm{GeV}/c$. *Phys. Rev. Lett.*. **81**, 5760-5763 (1998,12), https://link.aps.org/doi/10.1103/PhysRevLett.81.5760

[4] Adolph, C., et al., A. Odd and even partial waves of $\eta\pi^-$ and $\eta'\pi^-$ in $\pi^- p \to \eta^{(\prime)}\pi^- p$ at $191\,\mathrm{GeV}/c$. *Physics Letters B.* **740** pp. 303-311 (2015), https://www.sciencedirect.com/science/article/pii/S0370269314008685

[5] Wallner, S. Exploring the Strange-Meson spectrum with COMPASS in the reaction $K^- + p \to K^-\pi^-\pi^+ + p$. https://cds.cern.ch/record/2802793

[6] Ketzer, B., et al. Light-meson spectroscopy with COMPASS. *Progress In Particle And Nuclear Physics*. **113** pp. 103755 (2020,7), http://dx.doi.org/10.1016/j.ppnp.2020.103755

[7] Rodas, A., et al. Determination of the Pole Position of the Lightest Hybrid Meson Candidate. *Phys. Rev. Lett.*. **122**, 042002 (2019,1), https://link.aps.org/doi/10.1103/PhysRevLett.122.042002

[8] Kopf, B., et al. Investigation of the lightest hybrid meson candidate with a coupled-channel analysis of $\bar{p}p$-, $\pi^- p$- and $\pi\pi$-Data. *The European Physical Journal C.* **81** (2021,12), http://dx.doi.org/10.1140/epjc/s10052-021-09821-2

[9] S.-U. Chung, T. L. Trueman, *Phys. Rev. D.* **11**, 633 (1975). doi:10.1103/PhysRevD.11.633

[10] Aghasyan, M. et al. Light isovector resonances in $\pi^- p \to \pi^-\pi^-\pi^+ p$ at $190\,\mathrm{GeV}/c$. *Phys. Rev. D.* **98**, 092003 (2018)